Eye (2013) 27, 1233–1242

www.nature.com/eye

Medscape EDUCATION

Continuing Medical Education:

Analyses of shape of eyes and structure of optic nerves in eyes with tilted disc syndrome by swept-source optical coherence tomography and three-dimensional magnetic resonance imaging

K Shinohara, M Moriyama, N Shimada, N Nagaoka, T Ishibashi, T Tokoro and K Ohno-Matsui

Release date: 11 October 2013; Expiration date: 11 October 2014

This activity has been planned and implemented in accordance with the Essential Areas and policies of the Accreditation Council for Continuing Medical Education through the joint sponsorship of Medscape, LLC and Nature Publishing Group. Medscape, LLC is accredited by the ACCME to provide continuing medical education for physicians.

Medscape, LLC designates this Journal-based CME activity for a maximum of *1 AMA PRA Category 1 Credit(s)™*. Physicians should claim only the credit commensurate with the extent of their participation in the activity.

All other clinicians completing this activity will be issued a certificate of participation. To participate in this journal CME activity: (1) review the learning objectives and author disclosures; (2) study the education content; (3) take the post-test with a 70% minimum passing score and complete the evaluation at **www.medscape.org/journal/eye**; (4) view/print certificate.

Learning objectives

Upon completion of this activity, participants will be able to:

1. Describe optical coherence tomography (OCT) findings of the optic disc in eyes with tilted disc syndrome (TDS), based on a medical record review.
2. Compare eyes with non-highly myopic TDS with those with highly myopic TDS.
3. Describe three-dimensional magnetic resonance imaging (3D MRI) findings of the optic disc in eyes with TDS.

Authors/Editors disclosure information

Andrew J Lotery has disclosed the following relevant financial relationships: received grants for clinical research from: Novartis Pharmaceuticals Corporation. Served as an advisor or consultant for: Allergan, Inc. and Novartis Pharmaceuticals Corporation. Served as a speaker or a member of a speakers bureau for: Novartis Pharmaceuticals Corporation.
Kosei Shinohara has disclosed no relevant financial relationships.
Muka Moriyama has disclosed no relevant financial relationships.
Noriaki Shimada has disclosed no relevant financial relationships.
Natsuko Nagaoka has disclosed no relevant financial relationships.
Tatsuro Ishibashi has disclosed no relevant financial relationships.
Takashi Tokoro has disclosed no relevant financial relationships.
Kyoko Ohno-Matsui has disclosed no relevant financial relationships.

Journal CME author disclosure information

Laurie Barclay has disclosed no relevant financial relationships.

CLINICAL STUDY

Analyses of shape of eyes and structure of optic nerves in eyes with tilted disc syndrome by swept-source optical coherence tomography and three-dimensional magnetic resonance imaging

K Shinohara[1], M Moriyama[1], N Shimada[1], N Nagaoka[1], T Ishibashi[2], T Tokoro[1] and K Ohno-Matsui[1]

[1]Department of Ophthalmology and Visual Science, Tokyo Medical and Dental University, 1-5-45 Yushima, Bunkyo-ku, Tokyo, Japan

[2]Department of Ophthalmology, Kyushu University, Fukuoka, Japan

Correspondence:
K Ohno-Matsui,
Department of Ophthalmology and Visual Science, Tokyo Medical and Dental University,
1-5-45 Yushima,
Bunkyo-ku,
Tokyo 113-8510, Japan.
Tel: +81 3 5803 5302;
Fax: +81 3 3818 7188.
E-mail: k.ohno.oph@tmd.ac.jp

Received: 1 March 2013
Accepted in revised form: 14 May 2013
Published online: 11 October 2013

Abstract

Purpose **To evaluate the deeper structures of the optic nerve and to analyze the shape of eyes with tilted disc syndrome (TDS) by swept-source optical coherence tomography (OCT) and three-dimensional magnetic resonance imaging (3D MRI).**

Methods **The medical records of 54 eyes of 36 patients with TDS were reviewed. The patients with TDS and high myopia were analyzed separately from those without high myopia. All the eyes were examined with a swept-source OCT, and 22 of the eyes were examined by 3D MRI.**

Results **A total of 38 eyes of 29 patients were highly myopic and 16 eyes of 15 patients were not highly myopic. The representative OCT findings of the optic disc were: a sloping of the lamina cribrosa posteriorly from the upper part to the lower part, a protrusion of the upper edge of Bruch's membrane, and choroid. The distance and the depth of the most protruded point from the fovea were significantly greater in the eyes with non-highly myopic TDS than those with highly myopic TDS. In the 3D MRI, the lower part of the posterior segment was protruded outward, and the optic nerves attached at the upper nasal edge of the protrusion.**

Conclusions **The abnormalities detected by swept-source OCT and 3D MRI analyses indicate the possibility that the essential pathology of TDS is a deformity of the inferior globe below the optic nerve, and the positional relation between the fovea and the inferior protrusion determines the degree of myopia.**

Eye (2013) **27,** 1233–1242; doi:10.1038/eye.2013.202; published online 11 October 2013

Keywords: tilted disc syndrome; optic nerve; 3D MRI; swept-source OCT

Introduction

Tilted disc syndrome (TDS) has been thought to be a congenital anomaly caused by an incomplete closure of the fetal fissure of the eye, and it occurs in 1 to 2% of the populations.[1–5] The ophthalmic features of TDS include an inferonasal tilting of the optic disc, the presence of an inferior or inferonasal crescent, myopia, astigmatism, and an ectasia of the lower fundus or inferior staphyloma.[1–5]

Ectasia of the lower fundus or an inferior staphyloma is seen in 72 to 90% of TDS cases.[1,6] Young and associates examined one autopsy eye histologically and reported that the sclera appeared thinner below than above, suggesting an inferior ectasia.[7]

The optic disc abnormalities in TDS have been mainly analyzed by ophthalmoscopic examinations. A PubMed search using keywords 'tilted disc' and 'optical coherence tomography (OCT)' on 2 October 2012 extracted 13 articles. However, after excluding the myopic disc tilt, only seven studies examined TDS by OCT.[8–14] The purpose of OCT examination in six of these studies was limited to measuring the thickness of the peripapillary retinal nerve fiber layer or to analyzing the macular pathologies, for example, serous retinal detachment and choroidal neovascularization. It was not possible to observe the deeper structures within the optic nerve or the deeper tissues of the eye by conventional OCT.

The recent advancements in OCT instruments have enabled clinicians to examine the deeper structures of the eye.[15–18] The swept-source OCT has the capability of obtaining images of deeper structures, and this ability is made possible by using a wavelength-sweeping laser as the light source.[19]

A PubMed search identified two articles examining the shape of the eye with TDS *in situ*.[20,21] However, only one case was examined in each of these two studies, and conventional two-dimensional (2D) magnetic resonance imaging (MRI) was used. B-mode ultrasonography has also been used to detect the presence of inferior staphylomas in eyes with TDS,[22] however, the area that can be observed by ultrasonography is limited.

Recently, three-dimensional (3D) MRI has been shown to have the ability to obtain 3D images of human tissues, and we reported the characteristics of the shape of eyes with pathologic myopia obtained by 3D MRI analyses.[23] By modifying the signal intensity, it was also possible to view the retrobulbar optic nerve and the entire eye simultaneously.[23,24]

Thus, the purpose of this study was to evaluate the deeper structures of the optic nerve and also to measure the depth and distribution of inferior staphylomas in non-highly myopic and highly myopic eyes with TDS. To accomplish this, we examined highly myopic and non-myopic eyes with TDS by swept-source OCT. We also performed 3D MRI analyses to determine the shape of the eyes with TDS and analyzed an association between the eye shape and the attachment site of the optic nerve in patients with TDS.

Materials and methods

The procedures used in this research adhered to the tenets of the Declaration of Helsinki, and approval of the procedures used was obtained from the Ethics Committee of the Tokyo Medical and Dental University.

The medical records of patients with TDS who had an examination of the optic disc by swept-source OCT and stereoscopic fundus examinations were reviewed. All the patients were examined between January 2011 and August 2012. The diagnosis of TDS was made by stereoscopic fundus examination with an agreement of three of the authors (KS, KO-M, and MM). A diagnosis of TDS was made when the upper edge of the optic disc protruded anteriorly relative to its lower edge on stereoscopic fundus photographs (AFC-210, NIDEK Co., Ltd, Gamagori, Japan).[25] The patients with TDS and high myopia were analyzed separately from those without high myopia. The definition of high myopia was an axial length >26.5 mm. All patients underwent comprehensive ophthalmic examinations including measurements of the refractive error, axial length with the IOL Master (Carl Zeiss Meditec, Jena, Germany), dilated fundus examination, stereo fundus photography, and swept-source OCT. Fourteen of the patients were examined by 3D MRI.

Swept-source OCT examinations

All the eyes were examined with a swept-source OCT prototype instrument manufactured by Topcon Corporation (Tokyo, Japan). This OCT system has an A-scan repetition rate of 100 000 Hz, and its light source operates in the 1 μm wavelength region. The light source is a wavelength tunable laser centered at 1050 nm with a 100 nm tuning range. The axial resolution was measured to be 8 μm, the lateral resolution was 20 μm, and the imaging depth was 2.3 mm in tissues. Radial scans consisting of 12 equal meridian scans (scan length; 12 mm) centered on the optic disc were performed in all the 54 eyes. Also, the same radial scans centered on the fovea were performed in 24 eyes.

The most protruded part in the posterior fundus was identified in each of the 12 radial scans centered on the fovea, and the depth of the most protruded part from the foveal plane was measured in each scan as we reported (Supplementary Figure A).[24] Then, the scan that had the most protruded part was determined. The distance of the most protruded point from the fovea, and the depth of the most protruded point from the foveal plane were measured with the caliper function of the built-in software of the OCT (Supplementary Figure B).

3D high-resolution MRI

A MRI scanner (Signa HDxt 1.5T, version 15, GE Healthcare, Waukesha, WI, USA) was used with the following sequences. A fat suppressed T_2-weighted cube, which is an improved sequence of 3D fast-spin-echo with the following parameters: 256×256 matrix, 22 cm field of view, 1.2 mm slice thickness, repetition time 250 ms, echo time 90 ms, and echo train length 90. Volume renderings

of the images were generated from high-resolution 3D data on a computer workstation (v. AW 4.4, GE Healthcare).

The margins of the globes were detected semi-automatically by the signal intensity, and the tissues around the globes were carefully removed. Then, the optic nerves were identified by increasing the intensity with a removal of the surrounding tissues from time-to-time so that the optic nerves and the attachment sites were clearly observed. After obtaining the globes and the optic nerves, we evaluated the morphological features of the shape of eyes, site of attachment of the optic nerves to the globes, and how the optic nerves attach to the globes.

Statistical analyses

Student's *t*-tests were used to compare the average value of the distance and the depth of the most protruded point in the posterior segment from the central fovea. A *P*-value <0.05 was considered statistically significant.

Results

Fifty-four eyes of 36 patients with TDS were identified from their medical records and stereo fundus photographs. Among these 36 patients, 18 had bilateral TDS and the other 18 patients had unilateral TDS. There were 6 men and 30 women. The mean age of the patients was 68.0 ± 11.5 years with a range of 43–88 years. The mean axial length of the eyes with TDS was 27.5 ± 2.2 mm with a range of 23.3 to 32.1 mm, and the mean refractive error (spherical equivalent) was -8.6 ± 4.3 D with a range of -0.5 to -16.0 D excluding 15 eyes with implanted intraocular lens. Thirty-eight eyes of 29 patients were highly myopic and 16 eyes of 15 patients were not highly myopic. The clinical characteristics of these patients are shown in Table 1.

Swept-source OCT findings of optic disc

The OCT images of the optic discs in the eyes with TDS showed: a sloping of the lamina cribrosa posteriorly from the upper part to the lower part, a protrusion of the upper edge of Bruch's membrane and choroid, an elevation of the nerve fiber tissue at the upper margin of the optic disc (Figure 1). The inner laminar surface could not be clearly observed in 25 eyes because the tilting was too steep. A sloping of the inner laminar surface was observed in 27 of the 29 eyes (Figures 1a and b). At the upper edge of the optic disc, Bruch's membrane-choroid appeared to protrude toward the optic disc area (Figures 1c and d) in all the 54 eyes. The retinal nerve fiber tissue appeared to be herniated into the protruded Bruch's membrane and choroid in nine eyes (Figures 1c and d). In 30 eyes, the retinal nerve fiber tissue at the superior edge of the optic disc was elevated and protruded into the vitreous (Figures 1e and f). In addition to these features, an intrachoroidal cavitation (ICC) was detected at the lower optic disc in 13 of the 38 highly myopic eyes (34.2%; Figures 1g and h), but an ICC was not observed in any of the non-highly myopic eyes with TDS. The OCT findings in eyes with TDS with and without high myopia are summarized in Table 2.

Identification of most protruded point in eyes with inferior staphyloma

The 12 radial scans centered on the fovea delineated the curvature of the inner scleral surface precisely as we have reported.[24] The 12 radial scans centered on the fovea were obtained from 24 of 54 eyes, and the distance between the most protruded part and the fovea and the depth of the most protruded point from the foveal plane were identified in these 24 eyes. Nine of the 24 eyes were not highly myopic and the remaining 15 eyes were highly myopic. The clinical characteristics and the values of the most protruded point in both groups are shown in Table 3.

The most protruded point existed along the vertical section across the fovea in 11 eyes and existed 15 degrees inferotemporal to the fovea in the remaining eyes. The average distance between the most protruded point and the fovea was 3497.4 ± 763.3 μm with a range of 2237–4473 μm in 9 non-highly myopic eyes, and

Table 1 The eye and clinical characteristics of the patients with tilted disc syndrome with and without high myopia

	Highly myopic TDS	*Non-highly myopic TDS*
Gender. no. patients (eyes)	29 (38)	15 (16)
Men	5	2
Women	24	13
Age (y/o), mean ± SD (range)	66.1 ± 11.2 (43 to 86)	74.9 ± 9.3 (58 to 88)
Refractive error (D), mean ± SD (range)	−10.6 ± 2.5 (−6.5 to −16.0)	−3.1 ± 3.1 (0.5 to 7.3)
Axial length (mm), mean ± SD (range)	28.7 ± 1.3 (26.8 to 32.1)	24.9 ± 1.0 (23.3 to 26.3)
MRI acquisition (eyes)	14	8

Abbreviations: D, diopter; MRI, magnetic resonance imaging; SD, standard deviation; TDS, tilted disc syndrome; y/o, years old.

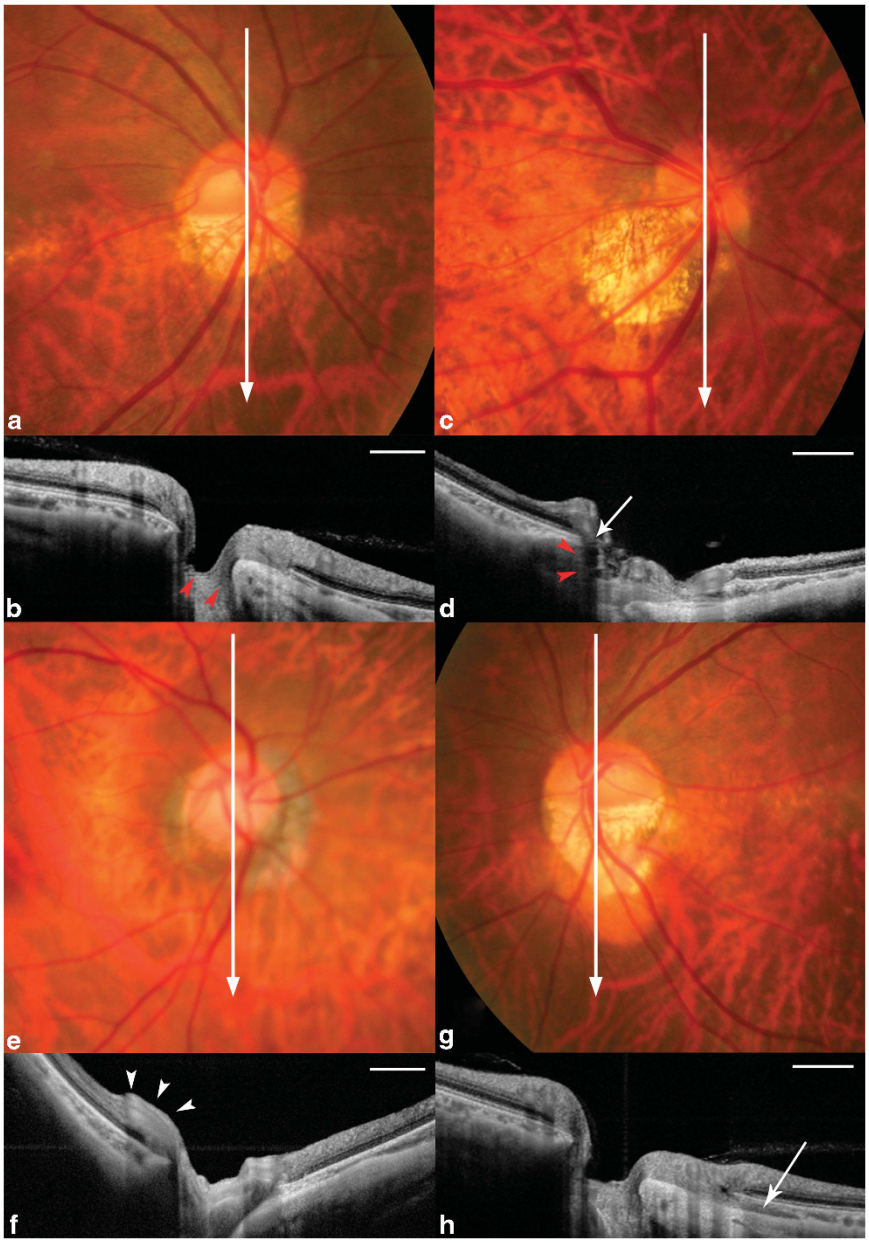

Figure 1 Fundus photographs and swept-source OCT images showing the characteristics of the OCT findings of the optic disc in the eyes with TDS. (a) Fundus photograph of the right eye of a 58-year-old woman with a refractive error (spherical equivalent) of −5.0 diopters and axial length of 26.3 mm. The optic disc is tilted inferiorly, and an inferior conus is present. The fundus inferior to the optic disc is tessellated. The OCT scan direction for Figure 1b is shown as a white line with arrowhead. (b) Vertical OCT image recorded along the white scan line in Figure 1a. The inner surface of the lamina cribrosa has a clear change of reflectance (arrowheads). The lamina is sloped posteriorly from the upper part to the lower part. (c) Fundus photograph of the right eye of a 60-year-old woman with a refractive error (spherical equivalent) of −12.5 diopters and axial length of 28.7 mm. The optic disc is tilted and a conus is present inferotemporal to the optic disc. The OCT scan direction for Figure 1d is shown as white line with arrowhead. (d) Vertical OCT image along the white line in Figure 1c. The Bruch's membrane-choroid complex is protruded (arrow) toward the optic disc area along the upper margin of the disc. The nerve tissue is herniated into the protruded Bruch's membrane-choroid complex and bent superiorly (arrowheads) beyond the upper margin of the optic disc. (e) Fundus photograph of the right eye of a 67-year-old woman with an axial length of 25.9 mm. The optic disc is tilted inferiorly. The OCT scan direction for Figure 1f is shown as white line with arrowhead. (f) Vertical OCT image across the optic disc showing that the retinal nerve fiber tissue is elevated (arrowheads) along the upper border of the optic disc. (g) Fundus photograph of the left eye of a 58-year-old woman with a refractive error (spherical equivalent) of −6.5 diopters and axial length of 27.1 mm. The optic disc is tilted and an inferior conus is present. The OCT scan direction for Figure 1h is shown as white line with arrowhead. (h) Vertical OCT image showing the presence of ICC (white line with arrowhead) inferior to the tilted optic disc. Scale bars = 1 mm.

Table 2 OCT findings of the optic disc area in eyes with tilted disc syndrome with and without high myopia

	Highly myopic TDS (38 eyes)	*Non-highly myopic TDS (16 eyes)*
Sloping of lamina cribrosa toward posteriorly	20/20 eyes[a]	7/9 eyes[a]
Protrusion of BM/choroid at the upper edge	38 eyes (100%)	16 eyes (100%)
Herniation of nerve tissue into beneath the protrusion	6 eyes (15.8%)	3 eyes (18.8%)
Elevation of nerve fiber tissue at the upper margin of the optic disc	21 eyes (55.3%)	9 eyes (56.3%)
Intrachoroidal cavitation	13 eyes (34.2%)	0 eyes (0%)

Abbreviations: BM, Bruch's membrane; OCT, optical coherence tomography; TDS, tilted disc syndrome.
[a] Limited to the eyes whose lamina was observed by OCT.

Table 3 The characteristics of the most protruded point in the posterior fundus in eyes with tilted disc syndrome with and without high myopia

	Highly myopic TDS	*Non-highly myopic TDS*	P-*value*
Number of eyes	15	9	
Refractive error (D), mean ± SD (range)	−10.4 ± 2.4 (−7.5 to −14.8)	−3.9 ± 3.6 (−0.5 to −7.3)	
Axial length (mm), mean ± SD (range)	28.1 ± 0.9 (26.8 to 29.5)	24.4 ± 0.8 (23.3 to 26.0)	
The distance between the most protruded point and the fovea (μm), mean ± SD (range)	2451.2 ± 691.5 (1195 to 4290)	3497.4 ± 763.3 (2237 to 4473)	0.002[a]
The depth of the most protruded point from the foveal plane (μm), mean ± SD (range)	611.5 ± 284.4 (207 to 1100)	935.8 ± 396.8 (537 to 1730)	0.03[a]

Abbreviations: D, diopters; SD, standard deviation; TDS, tilted disc syndrome; y/o, years old.
[a] Student's *t*-test.

2451.2 ± 691.5 μm with a range 1195–4290 μm in 15 highly myopic eyes. Similarly, the average depth of the most protruded point from the foveal plane was 935.8 ± 396.8 μm with a range of 537–1730 μm in the 9 non-highly myopic eyes and 611.5 ± 284.4 μm with a range of 207–1100 μm in the 15 highly myopic eyes. The differences in the distance and the depth of the most protruded point from the fovea between highly myopic and non-highly myopic TDS eyes were significant (Student's *t*-tests, $P = 0.002$ for distance; $P = 0.03$ for depth; Table 3).

Analysis of eye shape and attachment site of optic nerve to eye in 3D MRI

Eyes without TDS. There were 28 eyes (14 patients) that were examined by 3D MRI. There were six patients with unilateral TDS, and the fellow eyes of these six patients were used as controls without TDS. The mean axial length of these six eyes without TDS was 25.4 ± 2.7 mm with a range of 22.7 to 29.9 mm, and the mean refractive error was −1.0 ± 2.8 D with a range of +2.0 to −3.5 D. As we reported, in emmetropic eyes without any ophthalmic abnormalities, 3D MR imaging showed that the posterior segment of the eyes was almost hemispheric in shape without protrusions.[23] The attachment site of the optic nerve was slightly nasal from the center of posterior segment, and the optic nerve was attached perpendicularly to the globes. The curvature of the attachment site of the optic nerve was vertically straight when the globe was viewed from the nasal side. In the six eyes without TDS, two eyes were highly myopic and the remaining four eyes were emmetropic without any ophthalmic abnormalities. The 3D MR images of the four emmetropic eyes appeared to be approximately the same as that of normal emmetropic eyes (Figures 2a and b). In the other two eyes with high myopia, one eye had a protrusion along the visual axis and the other one eye had a protrusion in the lower part of posterior segment. Regardless of the location of protrusion area, the attachment site of the optic nerves was within the protrusion, and the optic nerve was attached perpendicularly to the globes (Figures 2c and d). The curvature of the attachment site of the optic nerve was vertically straight when the globe was viewed from the nasal side.

Eyes with TDS. The 3D MR images of 22 eyes with TDS were then analyzed. Among the 22 eyes, 14 eyes were highly myopic and 8 eyes were not highly myopic. All of the 22 eyes had common features of the shape of the globes and attachment site of the optic nerves regardless of being highly myopic or not. The lower part of the posterior segment was protruded, and the optic nerves attached at the upper nasal edge of the protrusion (Figures 2e and f). In all the 22 TDS eyes, the attachment site of the optic nerve was oblique when viewed from the nasal side. The lower half of the globe had a completely different curvature from the upper half of the eye in eyes with TDS (Figure 2e). Although the lower boundary of a staphyloma is usually apparent by 3D MRI in highly myopic eyes without TDS (Figure 2d), the expansion of lower globe is so extensive in the eyes with TDS that the

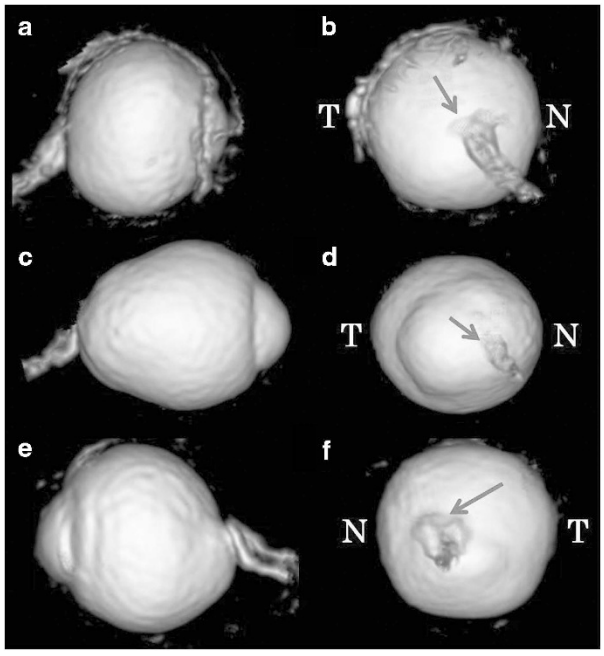

Figure 2 Spatial relationship between the attachment site of the optic nerve and the entire eye based on 3D MR images of eyes with and without TDS. (a, b) Nasal view (a) and posterior view (b) of an emmetropic eye. The axial length of the eye is 23.8 mm. The shape of the posterior segment of the eyes is symmetrically hemispheric. The attachment site of the optic nerve is slightly nasal from the center of the posterior segment (b, arrow), and the optic nerve is attached perpendicularly to the globe (a). The curvature of the attachment site of the optic nerve is vertically straight when the globe is viewed from the nasal side (a). (c, d) Nasal (c) and posterior (d) views of a highly myopic eye without TDS. Axial length of the eye is 29.9 mm. The eye is elongated in anterior–posterior direction and a posterior protrusion exists along with the visual axis (c). The attachment site of the optic nerve is in the middle of the protrusion (c, d arrow), and the optic nerve is attached perpendicularly to the globe (c). The curvature of the attachment site of the optic nerve is vertically straight when the globe is viewed from the nasal side (c). The lower boundary of the posterior protrusion can be clearly seen (d). (e, f) Nasal (e) and posterior (f) views of an emmetropic eye with TDS. Axial length of the eye is 23.7 mm. The lower half of the globe has a completely different curvature from the upper half of the eye (e). The expansion of lower globe is wide and the lower boundary of the inferior staphyloma is not obvious (f). The optic nerve is attached along the upper edge of posterior protrusion and the curvature of the attachment site of the optic nerve is oblique when the globe is viewed from the nasal side (e, f arrow). N, nasal; T, temporal.

lower boundary of inferior staphyloma was not clearly seen (Figures 2e and f).

Conclusion

Swept-source OCT examinations of the optic nerve in eyes with TDS showed various abnormalities, which appeared to be specific to TDS. First, the lamina cribrosa sloped posteriorly from the upper part to the lower part in most of the eyes with TDS (Figure 1b, lamina is visible by OCT). The lamina cribrosa is a part of the scleral tissue, and the principal part of the lamina cribrosa is formed by an extension of collagen bundles and elastic fibers from the inner two-thirds of the sclera across the optic nerve canal.[25] Jonas *et al*[26] reported that there was a significant correlation between the thickness of lamina cribrosa and the thickness of the peripapillary sclera. Considering these relationships, we can assume two possibilities. One possibility is that a sloping of the lamina cribrosa could affect the curvature of the peripapillary sclera, which might eventually progress to an inferior staphyloma. The other is that the sloping of the lamina cribrosa is a result of the protrusion of the lower globe.

Other OCT features of eyes with TDS were the protrusion of Bruch's membrane toward the optic nerve along its upper edge and the herniation of the retinal nerve fiber below the protruded Bruch's membrane and choroid (Figures 1c and d). As a result of this herniation, the retinal nerve fiber appeared to be acutely bent along the upper margin of the optic nerve head. It is well-known that the patients with TDS can develop visual field defects.[27] In most of the cases with TDS, the visual field defects were reduced or not present when corrective lenses are positioned corresponding to the floor of the ectatic fundus. Thus, these visual field defects are considered to be refractive scotomas.[25,28] However, it has also been reported that some visual field defects were not improved by an increase in the myopic correction.[28] Although the mechanism causing the visual field defects that were not improved by increased myopic correction has not been determined, it is possible that it is due to the severe bending of the retinal nerve fiber tissue, which would impair axonal flow. We did not thoroughly analyze the visual field in this study, so more comprehensive studies are necessary to determine this hypothesis.

An ICC was observed in 34.2% (13 of 38 eyes) of the highly myopic eyes with TDS. We have reported that an ICC was present in 5% of highly myopic eyes.[29] In addition, using EDI-OCT and swept-source OCT, we recently reported that the development of an ICC was accompanied by a stretching and defects of the border tissues of Jacoby.[30] ICCs almost always develop inferior to the optic disc, and even in large ICCs around the optic disc, the area inferior to the optic disc is always involved.[29] Considering the high incidence of ICCs in highly myopic TDS eyes, and the strong tendency of ICCs to develop inferiorly, the border tissue of Jacoby might be stretched and disrupted more easily in highly myopic eyes especially when they are associated with TDS. The tilting of the optic disc inferiorly can probably

accelerate the damage of the border tissues resulting in ICC formation.

Our 3D MRI analyses showed that the shape of eyes with TDS was asymmetrical between the upper and lower halves of the globe (Figure 2e). The posterior bulge of the inferior staphyloma was so extensive that the lower boundary of inferior staphyloma was not clearly recognized in the 3D MR images (Figures 2e and f). On the other hand, in highly myopic eyes without TDS, the area of the posterior staphyloma was smaller and the lower boundary was easily identified (Figure 2d). These findings suggest that the eye deformities caused by TDS affect a wider area of the globe than the eye deformities in highly myopic eyes without TDS.

The measurements of the swept-source OCT images showed that the most protruded point in the posterior fundus was significantly more posterior and farther from the fovea in eyes with non-highly myopic TDS than those with highly myopic TDS. These findings suggest that in eyes with highly myopic TDS, the protrusion of the lower globe include the fovea whereas it mainly occurs below the fovea in eyes with non-highly myopic TDS. When the fovea is not included in the protrusion of the lower globe and is not posteriorly dislocated, their axial length is not so long.

Our previous studies showed that even in highly myopic eyes without apparent features of TDS, the inferior sclera still tends to expand more than the other areas.[23,24] This suggests similarities in the developmental mechanism of eye deformities in eyes with TDS and with high myopia.

TDS is generally considered a congenital anomaly, which is due to a partial non-closure of the embryonic fissure.[1] However, owing to a lack of long follow-up data from childhood, it is unclear whether both the disc anomalies and inferior staphylomas co-exist at birth or whether the inferior staphyloma develops or deepens later in life. Although we have shown that the lamina cribrosa sloped posteriorly in the swept-source OCT images, it is not clear if this sloping of the lamina is a cause or a result or just a complication of an inferior staphyloma. Inferring from the similarities of the deformities in eyes with TDS and eyes with high myopia without TDS, the essential pathology of TDS might be a posterior bulge involving a wide area of inferior globe. The appearance of the optic disc might be influenced only by the relationship between the attachment site of the optic nerve and the upper edge of posterior bulge. These points need to be evaluated in a long-term longitudinal follow-up studies.

There are several limitations in this study. The number of the patients was not large especially the non-highly myopic eyes with TDS. The optic disc was examined by swept-source OCT in all the patients but the area centered on the fovea was not examined in all the patients. Not all the eyes with TDS were examined by 3D MRI. We carefully diagnosed TDS by a definition based on stereoscopic fundus photographs and the classification was determined by the agreement of three authors. However, it might be difficult to exclude the possibility that the myopic disc tilt (usually temporal or lower-temporal direction) because of high myopia was misdiagnosed as TDS in highly myopic TDS groups. Despite these limitations, we believe that the analyses of the optic disc and posterior scleral curvature by swept-source OCT, and the analyses of the shape of the eye by 3D MRI have provided important evidence for the development of TDS and how it affects the optic nerve.

In conclusion, we investigated the abnormalities of the deep structures in the optic nerve by swept-source OCT and also the shape of the eye by 3D MRI in eyes with TDS. Also, the eye deformity in the inferior fundus was common in both non-highly myopic TDS and highly myopic TDS. These informations should be useful in determining the pathogenesis of TDS.

Summary

What was known before

- TDS has been mainly analyzed by ophthalmoscopic examinations, and characterized by an inferonasal tilting of the disc, presence of an inferior or inferonasal crescent, myopia, astigmatism, and ectasia of the lower fundus, also referred to as an inferior staphyloma. But the deeper structure of the optic nerve and entire eye shape have not been clarified.

What this study adds

- Swept-source OCT and 3D MRI can clearly show the various abnormalities in the optic nerve and shape of the entire eye in the eyes with TDS.

Conflict of interest

The authors declare no conflict of interest.

Acknowledgements

We thank Professor Duco Hamasaki for his critical discussion and final manuscript revision.

References

1 Brown GC, Tasman W. *Congenital Anomalies of the Optic Disc. Excavated and colobomatous defects*. Grune & Stratton: New York, NY, USA, 1983, pp 95–192.
2 Alexander LJ. The tilted disc syndrome. *J Am Optom Assoc* 1978; **49**(9): 1060–1062.
3 Apple DJ, Rabb MF, Walsh PM. Congenital anomalies of the optic disc. *Surv Ophthalmol* 1982; **27**(1): 3–41.

4 Dorrell D. The tilted disc. *Br J Ophthalmol* 1978; **62**(1): 16–20.
5 Sowka J, Aoun P. Tilted disc syndrome. *Optom Vis Sci* 1999; **76**(9): 618–623.
6 Riise D. Visual field defects in optic disc malformation with ectasia of the fundus. *Acta Ophthalmol* 1966; **44**(6): 906–918.
7 Young SE, Walsh FB, Knox DL. The tilted disk syndrome. *Am J Ophthalmol* 1976; **82**(1): 16–23.
8 Moschos MM, Margetis I, Papadimitriou S, Moschos M. Clinical and multifocal-electroretinographic findings of congenital tilted disc syndrome associated with choroidal neovascularization: a case report. *Doc Ophthalmol* 2007; **115**(2): 121–124.
9 Milani P, Pece A, Moretti G, Lino P, Scialdone A. Intravitreal bevacizumab for CNV-complicated tilted disk syndrome. *Graefes Arch Clin Exp Ophthalmol* 2009; **247**(9): 1179–1182.
10 Hong S, Kim CY, Seong GJ. Adjusted peripapillary retinal nerve fiber layer thickness measurements based on the optic nerve head scan angle. *Invest Ophthalmol Vis Sci* 2010; **51**(8): 4067–4074.
11 Milani P, Pece A, Pierro L, Seidenari P, Radice P, Scialdone A. Bevacizumab for macular serous neuroretinal detachment in tilted disk syndrome. *J Ophthalmol* 2010; **2010**: 97058030; doi:10.1155/2010/970580.
12 Pardo-Lopez D, Gallego-Pinazo R, Mateo C, Rohrweck Sm Suelves AM, Dolz-Marco R *et al*. Serous macular detachment associated with dome-shaped macula and tilted disc. *Case Report Ophthalmol* 2011; **2**(1): 111–115.
13 Moschos MM, Triglianos A, Rotsos T, Papadimitriou S, Margetis I, Minogiannis P *et al*. Tilted disc syndrome: an OCT and mfERG study. *Doc Ophthalmol* 2009; **119**(1): 23–28.
14 Maruko I, Iida T, Sugano Y, Oyamada H, Sekiryu T. Morphologic choroidal and scleral changes at the macula in tilted disc syndrome with staphyloma using optical coherence tomography. *Invest Ophthalmol Vis Sci* 2011; **52**(12): 8763–8768.
15 Ohno-Matsui K, Akiba M, Moriyama M, Ishibashi T, Tokoro T, Spaide RF. Imaging the retrobulbar subarachnoid space around the optic nerve by swept source optical coherence tomography in eyes with pathologic myopia. *Invest Ophthalmol Vis Sci* 2011; **52**: 9644–9650.
16 Ohno-Matsui K, Akiba M, Moriyama M, Shimada N, Ishibashi T, Tokoro T *et al*. Acquired optic nerve and peripapillary pits in pathologic myopia. *Ophthalmology* 2012; **119**(8): 1685–1692.
17 Park HY, Jeon SH, Park CK. Enhanced depth imaging detects lamina cribrosa thickness differences in normal tension glaucoma and primary open-angle glaucoma. *Ophthalmology* 2012; **119**(1): 10–20.
18 Park SC, De Moraes CG, Teng CC, Tello C, Liebmann JM, Ritch R. Enhanced depth imaging optical coherence tomography of deep optic nerve complex structures in glaucoma. *Ophthalmology* 2012; **119**: 3–9.
19 Yun SH, Bouma BE. Wavelength swept lasers. Drexler W, Fujimoto JG (eds). *Optical Coherence Tomography; Technology and Applications*. Springer: New York, NY, USA, 2008; pp 359–378.
20 Manfre L, Vero S, Focarelli-Barone C, Lagalla R. Bitemporal pseudohemianopia related to the 'tilted disk' syndrome: CT, MR, and fundoscopic findings. *Am J Neuroradiol* 1999; **20**(9): 1750–1751.
21 Tarver-Carr ME, Miller NR. Tilted optic discs visualized by magnetic resonance imaging. *J Neuroophthalmol* 2006; **26**(4): 282–283.
22 Bottoni FG, Eggink CA, Cruysberg JR, Verbeek AM. Dominant inherited tilted disc syndrome and lacquer cracks. *Eye* 1990; **4**(Pt 3): 504–509.
23 Moriyama M, Ohno-Matsui K, Hayashi K, Shimada N, Yoshida T, Tokoro T *et al*. Topographical analyses of shape of eyes with pathologic myopia by high-resolution three dimensional magnetic resonance imaging. *Ophthalmology* 2011; **118**(8): 1626–1637.
24 Ohno-Matsui K, Akiba M, Modegi T, Tomita M, Ishibashi T, Tokoro T *et al*. Association between shape of sclera and myopic retinochoroidal lesions in patients with pathologic myopia. *Invest Ophthalmol Vis Sci* 2012; **53**(10): 6046–6061.
25 Hogan MJ. Optic nerve. *Histology of the Human Eye*. WB Saunders: Philadelphia, PA, USA, 1971; pp 527–606.
26 Jonas JB, Jonas RA, Jonas SB, Panda-Jonas S. Lamina cribrosa thickness correlated with peripapillary sclera thickness. *Acta Ophthalmol* 2012; **90**(3): e248–e250.
27 Brown GC, Tasman W. *Tilted Disc Syndrome. Congenital Anomalies of the Optic Disc*. Grune & Stratton: New York, NY, USA, 1983; pp 172–178.
28 Vuori ML, Mantyjarvi M. Tilted disc syndrome may mimic false visual field deterioration. *Acta Ophthalmol* 2008; **86**(6): 622–625.
29 Shimada N, Ohno-Matsui K, Yoshida T, Yasuzumi K, Kojima A, Kobayashi K *et al*. Characteristics of peripapillary detachment in pathologic myopia. *Arch Ophthalmol* 2006; **124**(1): 46–52.
30 Spaide RF, Akiba M, Ohno-Matsui K. Evaluation of peripapillary intrachoroidal cavitation with swept source and enhanced depth imaging optical coherence tomography. *Retina* 2012; **32**: 1037–1044.

Supplementary Information accompanies this paper on Eye website (http://www.nature.com/eye)

Medscape EDUCATION

Analyses of shape of eyes and structure of optic nerves in eyes with tilted disc syndrome by swept-source optical coherence tomography and three-dimensional magnetic resonance imaging

To obtain credit, you should first read the journal article. After reading the article, you should be able to answer the following, related, multiple choice questions. To complete the questions (with a minimum 70% passing score) and earn continuing medical education (CME) credit, please go to **www.medscape.org/journal/eye**. Credit cannot be obtained for tests completed on paper, although you may use the worksheet below to keep a record of your answers.

You must be a registered user on Medscape.org. If you are not registered on Medscape.org, please click on the new users: Free Registration link on the left hand side of the website to register.

Only one answer is correct for each question. Once you successfully answer all post-test questions you will be able to view and/or print your certificate. For questions regarding the content of this activity, contact the accredited provider, CME@medscape.net. For technical assistance, contact CME@webmd.net.

American Medical Association's Physician's Recognition Award (AMA PRA) credits are accepted in the US as evidence of participation in CME activities. For further information on this award, please refer to http://www.ama-assn.org/ama/pub/category/2922.html. The AMA has determined that physicians not licensed in the US who participate in this CME activity are eligible for *AMA PRA Category 1 Credits*™. Through agreements that the AMA has made with agencies in some countries, AMA PRA credit may be acceptable as evidence of participation in CME activities. If you are not licensed in the US, please complete the questions online, print the AMA PRA CME credit certificate and present it to your national medical association for review.

1. Your patient is a 65-year-old woman with TDS. Based on the medical record review by Shinohara and colleagues, which of the following statements about OCT findings of the optic disc is most likely correct?

- A The lamina cribrosa slopes anteriorly from the upper part to the lower part.
- B The lamina cribrosa slopes posteriorly from the lower part to the upper part.
- C There is protrusion of the lower edge of Bruch's membrane.
- D There is protrusion of the choroid.

2. Based on the medical record review by Shinohara and colleagues, which of the following statements about eyes with non-highly myopic TDS compared with those with highly myopic TDS is most likely correct?

- A Most of the eyes with TDS were not highly myopic.
- B Compared with the eyes with highly myopic TDS, those with non-highly myopic TDS had significantly less distance of the most protruded point from the fovea.
- C Compared with the eyes with highly myopic TDS, those with non-highly myopic TDS had significantly less depth of the most protruded point from the fovea.
- D The investigators concluded that the degree of myopia in eyes with TDS is determined by the positional relation between the fovea and the inferior protrusion.

3. Which of the following statements about 3D MRI findings of the optic disc in eyes with TDS is most likely correct?

- A The lower part of the posterior segment is protruded inward.
- B The upper part of the posterior segment is protruded outward.
- C Findings suggest that the essential pathology of TDS is a deformity of the inferior globe below the optic nerve.
- D The optic nerves are attached at the lower nasal edge of the protrusion.

Activity evaluation

1. The activity supported the learning objectives.

Strongly disagree				Strongly agree
1	2	3	4	5

2. The material was organized clearly for learning to occur.

Strongly disagree				Strongly agree
1	2	3	4	5

3. The content learned from this activity will impact my practice.

Strongly disagree				Strongly agree
1	2	3	4	5

4. The activity was presented objectively and free of commercial bias.

Strongly disagree				Strongly agree
1	2	3	4	5